Materials Science in Semiconductor Processing 85 (2018) 33–39

Contents lists available at ScienceDirect

Materials Science in Semiconductor Processing

journal homepage: www.elsevier.com/locate/mssp

Role of thermal treatment on sol-gel preparation of porous cerium titanate: Characterization and photocatalytic degradation of ofloxacin

Wenjie Zhang*, Jiao Yang, Chuanguo Li

School of Environmental and Chemical Engineering, Shenyang Ligong University, Shenyang 110159, China

ARTICLE INFO

Keywords:
$CeTi_2O_6$
Photocatalysis
Calcination
Ofloxacin
Degradation

ABSTRACT

$CeTi_2O_6$ was prepared using PEG4000 as template agent in a sol-gel route. Crystallization of brannerite structured $CeTi_2O_6$ begins at 700 °C, while phase transformation from $CeTi_2O_6$ to CeO_2 and rutile TiO_2 occurs in the samples calcined over 800 °C. The porous cerium titanate samples are composed of nano-sized spherical particles with interparticle holes. Ti-O and Ce-O bondings have characteristic absorptions in the FT-IR spectra of the crystallized samples. Band gap energies of the samples calcined at 500, 600, 700, 800, 900 and 1000 °C are 2.60, 2.61, 3.10, 3.18, 3.11 and 3.01 eV, respectively. Calcination temperature can put essential effect on the porous properties of the materials. BET surface area of the samples shrinks from 89 to 1.6 m^2/g when calcination temperature increases from 500° to 1000°C, accompanied with the decrease of total pore volume from 0.2849 to 0.0012 cm^3/g. The sample calcined at 800 °C has the maximum photocatalytic activity on both hydroxyl radical generation and ofloxacin degradation.

1. Introduction

Most hazardous organic substances in atmosphere and aquatic system can be removed through photocatalytic oxidation, which has grown to be an effective pollutant treating technique [1–3]. The most important research focus in this technique is the activity of photocatalyst, while different types of materials have been studied for this purpose in the past decades [4–6]. Besides the well-known TiO_2-based materials, titanate is a potential photocatalyst and has aroused much attention [7–11].

Titanates in perovskite and ilmenite structures are used as dielectric materials. The variation of cation element may not alter the crystalline structure of these materials, although elemental composition may influence the dielectric constant. Lanthanide titanates have showed their photocatalytic activity recently. Photocatalytic splitting of water was reported on $Gd_2Ti_2O_7$ and $Y_2Ti_2O_7$ [12]. Methyl orange was decomposed on pyrochloro structured $Nd_2Ti_2O_7$, $Gd_2Ti_2O_7$ and $Er_2Ti_2O_7$ [13]. Otsuka-Yao-Matsuo et al. reported photocatalytic behavior of cerium titanates, $CeTiO_4$ and $CeTi_2O_6$ [14]. Verma et al. studied microstructure, photocatalysis and electrochemical properties of $CeTi_2O_6$ thin films [15].

The desired activity of lanthanide titanates depends on crystallization processes in hydrothermal, solid state reaction, sol-gel and polymerized complex methods. High temperature thermal treatment is necessary for crystal formation. As a result, porous structure can hardly be found in these materials. Polyethylene glycol (PEG) is a long-chain macromolecular compound that can be used as template agent to modify the porous property of materials [16]. The addition of PEG can produce pores in many materials after thermal treatment, and can also put effect on crystal formation [17]. We reported enhanced photocatalytic activity of $La_2Ti_2O_7$ modified with PEG4000 in a sol-gel route [18].

PEG4000 was used to prepare $CeTi_2O_6$ in the sol-gel synthesizing process in this work. The effects of thermal treatment on the properties of cerium titanate were studied. The materials were characterized using scanning electron microscopy (SEM), transmission electron microscopy (TEM), X-ray powder diffraction (XRD), Fourier transform infrared/far infrared spectroscopy (FT-IR/FIR), UV–Visible spectrometry, fluorescence spectrophotometry, and surface area and pore analyses. Photocatalytic degradation of ofloxacin was measured in the lab-scale reactor to show the effect of thermal treatment on the activity of the cerium titanates.

2. Experimental

2.1. Preparation of cerium titanate

Cerium titanate was prepared through a sol-gel route. The first solution was composed of 8 mL ethanol and 0.85 mL tetrabutyl titanate, and the second solution was made from 8 mL deionized water, 3.5 g

* Corresponding author.
E-mail address: wjzhang@aliyun.com (W. Zhang).

https://doi.org/10.1016/j.mssp.2018.05.035
Received 21 November 2017; Received in revised form 17 May 2018; Accepted 27 May 2018
1369-8001/

PEG4000, 8 mL acetic acid and 0.4652 g $Ce(NO_3)_3{\cdot}6H_2O$. The two solutions were mixed together to form the sol under magnetic stirring. After 2 mL glycol was added later as a stabilizer, the sol was stirred in a water bath at 70 °C until the formation of gel. The gel was dried at 110 °C for 15 h in a furnace and was ground into fine powders. The subsequent thermal treatment was conducted for 3 h in an oven, whose temperature was increased from room temperature to 500–1000 °C at a heating rate of 5 °C/min. The product was ground again before use.

2.2. Characterization of the material

The surface morphologies of the materials were measured by QUANTA 250 scanning electron microscope and FEI Tecnai G2 20 transmittance electron microscope. X-ray powder diffraction patterns were taken on D8 X-ray diffractometer equipped with Cu Kα radiation. Infrared and far infrared absorption spectra were determined by Frontier FT-IR/FIR spectrometer. Specific surface area and pore size distribution were examined on ASAP 2460 surface area and pore size analyzer. The specific surface area was calculated using the multipoint Brunauer–Emmett–Teller (BET) method. Pore size distribution was calculated using the Barrett, Joyner, and Halenda (BJH) method. UV–Vis diffuse reflectance spectra were recorded by LAMBDA 35 UV–Vis spectrometer. An integrating sphere was equipped to determine the reflectance intensity. Kubelka-Munk method was used to transform reflection intensity to absorbance [19]. The scanning speed was 480 nm/min in the wavelength range between 200 and 700 nm. Differential scanning calorimetry (DSC) and thermogravimetric analysis (TGA) were taken on TA SDT Q600 simultaneous DSC-TGA heat flow analyzer.

2.3. Photocatalytic reaction

Photocatalytic degradation of ofloxacin was measured in a lab-made quartz reactor to evaluate the activity of cerium titanate. The 20 W lamp had an irradiation intensity of 2300 μW/cm^2 at 253.7 nm, which was measured at the surface of the solution. The initial pH of ofloxacin solution was 6.5 and the solution was used without adjustment. 20 mg photocatalyst and 50 mL 20 mg/L ofloxacin solution were stirred in the dark for 30 min to ensure adsorption-desorption equilibrium in order to measure adsorption percentage of ofloxacin on the material. Subsequently, the solution was illuminated for 30 min. The solution was centrifuged and filtrated to remove the solid photocatalyst powders. Ofloxacin concentration was measured using Agilent 1260 high performance liquid chromatography equipped with a ZorbaxEclipse XDB-C18 (150 × 4.6 mm, 5 μm) column. The mobile phase was made from 1% phosphoric acid aqueous solution and acetonitrile at a volume ratio of 80:20. The absorption intensity of ofloxacin at 294 nm was detected by a UV detector.

Hydroxyl radicals produced under 30 min illumination were determined in the suspension containing the photocatalyst and 50 mL 0.5 mmol/L terephthalic acid solution. After solid-solution separation, the solution was excited at 315 nm in LS-55 fluorescence spectrophotometer. The fluorescence intensity of 2-hydroxy-terephthalic acid was measured in the wavelength range between 350 nm and 550 nm.

3. Results and discussion

3.1. Characterization of $CeTi_2O_6$

Fig. 1 presents XRD patterns of cerium titanates calcined at different temperatures. High temperature thermal treatment is essential to crystallization of cerium titanate. The samples calcined below 600 °C are in the amorphous phase, while crystallization of brannerite structured $CeTi_2O_6$ begins at 700 °C. The brannerite structured $CeTi_2O_6$ is the only phase existing in the diffraction pattern at this temperature. Diffraction intensity of $CeTi_2O_6$ becomes stronger at higher temperatures up to 900 °C, as well as the formation of crystallite CeO_2 and rutile TiO_2 in the samples. The diffraction intensities of both CeO_2 and rutile TiO_2 increase with rising calcination temperature. Phase transformation from $CeTi_2O_6$ to CeO_2 and rutile TiO_2 is favored by high temperature thermal treatment. As a result, the sample calcined at 1000 °C is composed of CeO_2 and rutile TiO_2. The $CeTi_2O_6$ crystallite size is calculated from the preferred (110) plane using Scherrer formula. The crystallite sizes are 26.1, 38.0 and 50.2 nm for the samples calcined at 700, 800 and 900 °C, respectively. There might be a crystal growing tendency at high calcination temperature. Crystallite size of the material calcined at 1000 °C was also calculated for CeO_2 at the most preferred orientation (2θ = 28.5), and the crystallite size of CeO_2 is as large as 62.5 nm.

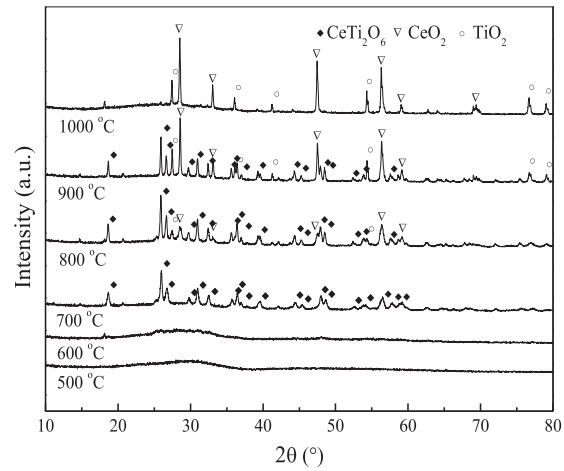

Fig. 1. XRD patterns of cerium titanate calcined at different temperatures.

Fig. 2 shows SEM surface morphologies of cerium titanate samples calcined at different temperatures. All the samples can be regarded as the aggregated small particles. The particles of the amorphous sample calcined at 500 °C are larger than the crystallized $CeTi_2O_6$ samples. There might be interparticle holes among the small $CeTi_2O_6$ particles in the samples calcined at 800 °C and 900 °C. Phase transformation from $CeTi_2O_6$ to CeO_2 and rutile TiO_2 at 1000 °C leads to enlarging particle size. Fig. 3 gives the high resolution TEM images of porous cerium titanate samples calcined at 500, 800 and 1000 °C. It can be seen from the images that the material is composed of nano-sized particles with interparticle holes. The particles have spherical shape and smooth surface. The boundaries of the particles get distorted at high temperature as the particles get fused into each other. The formation of interparticle holes can be related to the addition of PEG4000 template in the precursor [18].

FT-infrared and far infrared spectra of porous cerium titanate as a factor of calcination temperature are shown in Fig. 4. The absorption peaks at 3440 cm^{-1} and 1631 cm^{-1} belong to the surface adsorbed water. The stretching and bending vibrations of hydroxyl group shrink with increasing calcination temperature. Weak bending vibration absorption peaks of C-H at 1442 cm^{-1} and 1032 cm^{-1} are attributed to the organic residues in the materials [7]. Bending vibration of Ti-O bond has absorption at 670 cm^{-1} [7], and stretching vibration of Ti-O-Ti bond has a strong absorption peak at 514 cm^{-1} [20].

Absorption of metal oxide bonding can be distinguished in the far infrared spectra, as shown in Fig. 4(b). The amorphous samples calcined below 600 °C do not have apparent absorptions in the spectra. Metal oxide bonding has characteristic absorption in the spectra of the